Scientia Horticulturae 272 (2020) 109328

Contents lists available at ScienceDirect

Scientia Horticulturae

journal homepage: www.elsevier.com/locate/scihorti

Canopy cover evolution, diurnal patterns and leaf area index relationships in a Mchare and Cavendish banana cultivar under different soil moisture regimes

Bert Stevens[a,*], Jan Diels[b], Eline Vanuytrecht[b,f], Allan Brown[c], Stanley Bayo[c], Alvin Rujweka[d], Emmanuel Richard[c], Patrick Alois Ndakidemi[d], Rony Swennen[a,c,e]

[a] KU Leuven, Department of Biosystems, Willem De Croylaan 42 - Box 2455, 3001, Heverlee, Belgium
[b] KU Leuven, Division of Soil and Water Management Celestijnenlaan 200e - Box 2411, 3001, Leuven, Belgium
[c] International Institute of Tropical Agriculture, IITA, PO Box 447, Arusha, Tanzania
[d] Nelson Mandela African Institution of Science and Technology, NMAIST, P.O.BOX 447, Arusha, Tanzania
[e] Bioversity International, Willem De Croylaan 42, 3001, Heverlee, Belgium
[f] Flemish Institute for Technological Research (VITO), Environmental Modelling Unit, Boeretang 200, 2400 Mol, Belgium

ARTICLE INFO

Keywords:
Banana
Canopy cover
Leaf area index
Soil moisture deficit
Irrigation
Drone imagery

ABSTRACT

The biggest abiotic threat to banana (*Musa* spp.) production is water deficit, but physiological indicators in plantations are lacking. Canopy Cover (CC) seems to be a relevant parameter, but so far not used in banana fields. Field experiments were conducted to determine the effect of optimal irrigation (FI) versus rainfed (RF) on CC and Leaf Area Indices (LAI) in two experiments with different cultivars (Mchare 'Huti Green' [HG, AA] and Cavendish 'Grand Naine'[GN, AAA]) (n = 3 for HG, n = 4 for GN) until harvest of cycle 1 (C1), studying C1 and C2 plants. Soil moisture was followed using Time Domain reflectometry. CC and LAI were reduced 8–9 weeks after the start of soil moisture divergence between RF and FI treatments in both experiments ($p < 0.05$), leading to a reduction in CC growth rate (r) and maximum CC (CC_{max}) in RF plots ($p < 0.05$). On a daily timescale, CC varied diurnally (i.e. was reduced) under high evaporative demands, whereby soil moisture depletion increased the CC reduction. Cultivar specific CC-LAI curves were created following the Lambert-Beer equation, whereby HG had a lower extinction coefficient than GN (0.52 vs. 0.67). CC growth over time seems a promising indicator for water deficit in the field. Diurnally, CC is more affected by evaporative demand than soil moisture depletion, although soil moisture depletion increases CC diurnal drops under high ET_0.

1. Introduction

By 2050, global population levels are expected to reach 9.7 billion (+ 32 % from 2015), with over two thirds of this expansion happening in developing countries, and sub-Saharan Africa (SSA) accounting for half the total growth (United Nations., 2019). To feed this growing population, food production needs to increase by 25–70 % (Hunter et al., 2017; FAO., 2018). One of the most important crops in terms of consumption, land area and production is banana (*Musa* spp.). Global production of banana and plantains was 153 million Mg in 2017 covering 5.6 million ha in over 135 countries. It is the 12th most important food crop in terms of production (fourth in Africa) and the world's most important fruit (FAOSTAT, 2019).

In East and Central Africa (ECA), daily per capita consumption is 15 times the global average, and constitutes a very significant portion of daily energy intake ranging from 30 to 60 % (Abele et al., 2007; FAOSTAT., 2019). Actual production in the area is low (< 30 Mg ha^{-1} yr^{-1}) compared with attainable yields (> 70 Mg ha^{-1} yr^{-1}) (Wairegi et al., 2010; Van Asten et al., 2011). Water is the primary limiting factor for agriculture in SSA, where only 18 % of the total irrigable land is currently irrigated (Adhikari et al., 2015). Water (both excess and deficit) is considered to be the largest limiting abiotic factor affecting

Abbreviations: C1, cycle 1; C2, cycle 2; CC, canopy cover; CC_{ini}, initial canopy cover; CC_{max}, maximum canopy cover; CC_{rel}, relative CC; RF, rainfed; Dr, soil moisture depletion; ET_0, daily reference evapotranspiration; FC, field capacity; FI, full irrigation; GN, grande naine; HG, huti green; LA, leaf area; laf, leaf area factor; LAI, leaf area index; MAP, months after planting; nls, non-linear least squares; p, depletion factor; P, leaf pruning event; PWP, permanent wilting point; r, canopy cover growth rate; RAW, readily available water; TAW, total available water; VWC, volumetric water content; WAP, weeks after planting

* Corresponding author.
E-mail address: bert.stevens@kuleuven.be (B. Stevens).

https://doi.org/10.1016/j.scienta.2020.109328
Received 28 October 2019; Received in revised form 5 February 2020; Accepted 27 February 2020

banana production worldwide (Carr, 2009). Depending on the prevailing climate, water needs for banana range from 1100 to 2650 mm evenly distributed per year (Robinson and Alberts, 1986; Van Asten et al., 2011; Varma and Bebber, 2019). Even distribution is essential, as plants are already affected after two to three days of soil moisture deficit (Carr, 2009).

By 2050, climate change in ECA is expected to increase the thermal suitable area for banana production by 1–11 %, but extension of land area under beneficial temperatures is expected to be offset by an increase in rainfall variability. Moreover, as temperature drives development rates of banana (Fortescue et al., 2011), the increase in temperature is coupled with faster crop cycles, an increase in evapotranspiration, thereby increasing transpiration rates and putting more pressure on water resources (Adhikari et al., 2015; Varma and Bebber, 2019).

In view of the above, agriculture needs to be intensified by a more efficient use of both rainfall and irrigation water, and the enhancement of water use efficiency. In most cases, management of irrigation systems is based on farmers' intuition and experience, which is suboptimal (Boesveld et al., 2011), rather than allocating water when plants are in need. This is because easy physiological indicators for water deficit are lacking in banana, and most farmers find current irrigation scheduling tools overwhelming and lack the means and skills to install and operate them (Carr, 2009; Boesveld et al., 2011). Under relatively mild soil drought conditions, banana plants close their stomata, reduce transpiration and photosynthesis. This keeps leaves hydrated, most likely through root pressure, but masks that banana are under water deficit (Turner et al., 2007; Carr, 2009).

Expanding tissues, as emerging leaves and growing fruit, are among the first to be affected (Kallarackal et al., 1990; Thomas and Turner, 1998; Carr, 2009; Robinson and Galán Saúco, 2010). At the field (plantation) level, canopy development can be measured by the leaf area index (LAI) or green canopy cover (CC). LAI is defined as the total one-sided leaf area of all leaves per unit ground area ($m^2\ m^{-2}$). LAI values in banana plantations range from zero at planting to five at maturity in well-managed plantations, even reaching values more than six in ratoon crops (Turner, 1998; Turner et al., 2007; Carr, 2009). It is measured directly or indirectly. When leaves and plant parameters are measured directly, the most accurate LAI is obtained, but given the spatial heterogeneity of the canopy, many sampling points are needed which is time consuming, tedious, and sometimes destructive (Weiss et al., 2004). Indirect measurements are based on the estimation of "contact frequency" or the "gap fraction" with various possible optical devices (LAI2000, TRAC, Demon and cameras for hemispherical photography). Contact frequency methods are based on the likelihood that a beam penetrating the canopy will reach a vegetative structure. Gap frequency methods are inverse, as the beam has no contact with the vegetative structure until reaching a reference level and consequently the gaps in the canopy are measured. These techniques therefore use light transmittance through the canopy. Indirect methods need to be calibrated to the specific architecture of banana plants, as they are based on canopy characteristics such as leaf angle distribution, leaf inclination function and planting density (Weiss et al., 2004). Hence, indirect LAI methods are difficult to use when not yet parameterized and given the widespread heterogeneity of banana plants in the field, parameterization of LAI measurements for one cultivar at a specific location might not be useful in other plantations or fields with another cultivar.

A simpler indicator is the CC, defined as the proportion (%) of ground area covered by the vertical projection of the canopy (Jennings et al., 1999). In contrast to LAI, CC is easier to estimate given current drone technology. CC can easily and reliably be determined from image analysis. Unlike LAI, remote sensing and drone imagery allows a dynamic view of the CC averaged over much larger areas, as repeated images can be gathered at multiple times during the day of a complete plantation. This dynamic view of plantations is needed as individual banana plants unfold their lamina differently in response to variable environmental stimuli and soil conditions, typically following a diurnal rhythm with leaf halves forming a single plane aligned with the midrib during the night and early morning, and folding down to become more vertical during the day under periods of high radiation (Milburn et al., 1990; Thomas and Turner, 1998; Turner, 1998; Turner and Thomas, 1998; Turner et al., 2007). Lamina folding occurs in drought stressed plants (Milburn et al., 1990; Thomas and Turner, 1998; Turner and Thomas, 1998), but this is questioned (Lu et al., 2002). While the effect of drought on leaf emission and growth has been described (Turner and Thomas, 1998; Turner et al., 2007; Carr, 2009), the overall effect on CC, and therefore at the plantation level, is not known. Furthermore, the diurnal effect of leaf folding measured by CC cannot be reflected at the plantation scale by LAI as leaf sizes remain quite similar on a daily scale.

Given the lack of knowledge on CC in banana plantations, the overall objective was to investigate to what extent plot-scale observations of CC provide insights into water deficit. We hypothesize that soil moisture readily affects CC development as emerging leaves are among the first organs to be affected by drought. In addition we hypothesize diurnal changes in CC which are correlated with changes in daily evaporative demand, and that these changes are larger in plants experiencing water deficits. Thirdly, we hypothesized that CC-LAI relationships can be obtained per cultivar, allowing to calculate CC values from LAI values.

2. Materials and methods

2.1. Experimental site and conditions

Experiments were conducted at the joint research farm of the Nelson Mandela African Institution of Science and Technology (NM-AIST) and the International Institute of Tropical Agriculture (IITA) in Arusha, Tanzania (3° 23′ 58″ S, 36° 47′ 48″ E). Soils are Endocalcic Phaeozems (Geoabruptic, Clayic, Humic) (IUSS Working Group WRB., 2014) or Udertic to Vertic Haplustols (USDA., 1999) on gently sloping land (3%) located at the foothill of Mt. Meru at an altitude of 1188 m asl. Soils are moderately shallow to deep (90–120 cm), well structured, well drained with a silty clay loam to silty clay texture (Table S1).

The climate is a tropical highland climate with a moderately cool thermal zone (FAO, 2012). Rainfall follows a bimodal yearly pattern with a long rainy season extending from late March to early June and a shorter rainy season from October to December (Grieser et al., 2006). An automated weather station (TAHMO weather station: Decagon DS-2 sonic anemometer with pyranometer, REC-1 rain gauge, and VP-4 thermometer and humidity sensor with a solar-powered and GPRS-enabled EM50 G), located at the edge of the field, measured air temperature (°C), wind speed at 2 m height ($m\ s^{-1}$), relative humidity (%), precipitation (mm) and solar radiation ($MJ\ m^{-2}\ min^{-1}$) at a 5 min interval. Daily reference evapotranspiration (ET_0) was computed using the FAO Penman-Monteith approach (Allen et al., 1998). Daily weather variables of the entire experimental run can be found in supplementary data (Fig. S1).

2.2. Plant material

Banana plantations are composed of individual plants often of different reproductive cycles each growing on individual mats. When referring to a "plant" we refer to an individual reproductive cycle. When referring to a "mat", we refer to the total composition of different reproductive cycles present in one location. Generally, there are maximally three cycles present on a mat: a mother plant or cycle 1 (C1), a daughter plant or cycle 2 (C2) and a granddaughter plant or cycle 3 (C3). Our research focused on C1 and C2.

Two experiments were carried out differing only in cultivar and date of planting.

In experiment 1, the East African Highland banana Huti Green (HG, *Musa* AA Mchare subgroup; (Perrier et al., 2018)) was planted on 3 May 2017. In experiment 2, Grande Naine (GN, *Musa* AAA Cavendish subgroup) was planted on 17 November 2018. Planting material for both experiments consisted of *in vitro* plants, hardened in growth chambers and screenhouses. Plant height of HG at planting was 6.6 cm (± 2.5 cm), with 4.19 leaves (± 1.3 leaves), whilst plant height of GN was 25.5 cm (± 4.3 cm) and leaves were 4.75 leaves (± 0.74 leaves). Plant holes were 0.6 m × 0.6 m × 0.6 m deep at a spacing 2 m (row) × 3 m (line) (1666 plants ha^{-1}). Time is noted in weeks after planting (WAP). In following sections, the different experiments are noted by the planted cultivar (HG vs. GN). Experimental design, management and plant measurements were similar in both experiments unless stated otherwise.

2.3. Experimental design

The experiments were conducted on fields with no recent history of banana cultivation. The design was a blocked design with drip irrigation as treatment, but given the infrastructure the irrigation treatments could not be randomized.

In experiment 1, two blocks were planted with HG. Each block contained five rows of 15 mats, subdivided in three plots of 25 mats (5 × 5), of which the central nine mats (3 × 3) were used for data collection. Each block consisted of a different irrigation treatment, as valves to shut off irrigation were installed at the front of each block. For HG, there were three plots for each treatment. Border mats were used for periodic destructive sampling.

In experiment 2, four blocks were planted with GN. Each block contained five rows of 14 mats, subdivided in two plots of 35 mats (7 × 5), receiving two different irrigation treatments. Valves were installed in the middle of a plant row (between mat 7 and 8), therefore two irrigation treatments were present in a block. The central nine mats (3 × 3) were used for growth data collection, leading to four replications (plots) per treatment. The first and last two mats of each row (2 × 5 mats) together with the border rows were used for destructive sampling. Each treatment was replicated four times across the blocks.

2.4. Management

Mats received a mixture of mineral fertilizers and manure. Mineral fertilizers were split applied: 153 kg N ha^{-1} yr^{-1}(urea), 206 kg K ha^{-1} yr^{-1} (Muriate of potash), 19.26 kg Mg ha^{-1} yr^{-1} and 25.6 kg S ha^{-1} yr^{-1} ($MgSO_4$) were applied monthly in the rainy season and every two months in the dry season, while 40.2 kg P ha^{-1} yr^{-1} (triple super phosphate) was applied every five months. Twenty L of fresh farmyard cow manure was applied per mat twice yearly before the start of the rainy season. All suckers were allowed to grow until four months after planting (MAP), at which time one sucker of 30 cm height was selected and the others pruned. Each banana mat thereafter was composed of C1 and C2, and de-suckering was carried out afterwards on a monthly basis. Weeds and dead leaves were cut monthly and removed from the field.

Three additional leaf pruning events (P) occurred due to the development of Black Sigatoka (*Pseudocercospora fijiensis*) in the long wet season of 2018 at 2018-05-21 (P1), 2018-06-05 (P2), and 2018-07-30 (P3). At P1 and P2, only the oldest leaves with symptoms of the fungus (yellowing and petiole collapse) were cut. At P3 the oldest six leaves of each plant were cut away to retain the spread of the fungus affecting the older leaves.

2.5. Soil moisture and irrigation

Each banana row was fitted with two driplines, at each side of a banana mat. Originally each mat's position was fitted with two drippers (one at each side of the mat). Each dripper supplied approx. 4 l hr^{-1}. Two extra drippers were installed on 6 June 2018. For the HG experiment, this was at 57 WAP and for the GN experiment at 29 WAP.

Soil moisture was monitored daily by Time Domain Reflectometry (TDR). Within each plot, the central mat was fitted with two TDR probes installed vertically at different depths: 0 − 30 cm (horizon 1) and 30 − 60 cm (horizon 2). TDR probes were installed in the area wetted by the drippers, at 50 cm from the central mat and read out each morning before irrigation by a TDR-200 (Campbell scientific, Inc.). Daily moisture depletion, *Dr* (mm), was calculated at the plot level as:

$$Dr, i = 1000(\theta_{FC} - \theta_i) \times Z_r \quad (1)$$

with *Dr,i* being depletion on day i, θ_{FC} being the volumetric water content (VWC) at field capacity (FC, [m^3 m^{-3}]), θ_i being the actual VWC at day i (m^3 m^{-3}) and Z_r being the rooting depth (m). The rooting depth was estimated as a linear interpolation between the depth at 10 days after planting (0.1 m) and at flowering (1 m). Rooting depths were checked every three months over the course of the growing season through root trenching methods. Banana reaches a maximum rooting depth at flowering (Turner et al., 2007), and trenches revealed that roots were continually present until depths of 1 m after flowering in both HG and GN mats, as the soil profile was bounded by a saprolite hardpan layer at 1 m. Depletion values are positive when water contents are below FC and negative when values are above FC.

Daily depletion values were compared against the readily available water (RAW [mm]), as an indicator of moisture deficit. RAW was calculated as:

$$\text{RAW} = 1000(\theta_{FC} - \theta_{pwp}) \times Z_r \times p = TAW \times p; \quad (20)$$

with θ_{pwp} being the VWC at Permanent wilting point (m^3 m^{-3}), p being a depletion factor (-) and TAW being the total available water (mm). The value of p was chosen to be the generic factor of 0.35 for banana as given by Allen et al. (1998). When the $D_{r,i} > RAW$, plants are assumed to experience moisture deficit.

All mats received irrigation until 4 MAP (establishment period). Thereafter, two irrigation treatments were installed: optimal "full" irrigation (FI) and rainfed (RF). In the FI treatment, mats received water whenever more than 25 % of TAW was depleted in the first or second soil horizon. Water in the RF treatment was shut off after 4 MAP.

2.6. Banana growth measurements

Non-destructive plant growth data were measured monthly at the plot level (3 × 3 mats), on individual plants (C1 and C2) present on the mat until harvest of C1 as this corresponds to a CC growth cycle. Every three months, mats (n = 3) were selected in each treatment in both experiments for destructive sampling. Measured variables and variables calculated from growth measurements are listed in supplementary Table 2. As measurements continued on the same plants over time, the data required a repeated measures analysis of variance.

2.6.1. Canopy cover

CC was determined monthly for each plot, to assess the CC evolution over time. Before November 2017, when plants were small, images were taken at the individual mat level and CC was determined as an average of the CC of mats present in a plot. From November 2017 onwards, digital photographs of every plot were taken with a DJI-phantom 4 Pro drone (JPEG, image format, 20 M P, 4000 × 2250 pixels, and 72 dpi) at a height of 35 m above the ground with the center of the plot aligning to the center of the image. Before images were taken, the soil surface was weeded and residues removed.

To assess the influence of timing on diurnal CC patterns, CC pictures were taken at an hourly interval between 8 h and 16 h at nine different dates in both experiments: 2018-01-09, 2018-03-08, 2018-04-05, 2018-05-15, 2018-06-14, 2018-08-06, 2018-08-28, 2018-11-28 and 2018-12-17. CC values from the same plots taken at the same day were compared across different time points to assess the effect of timing on CC values.

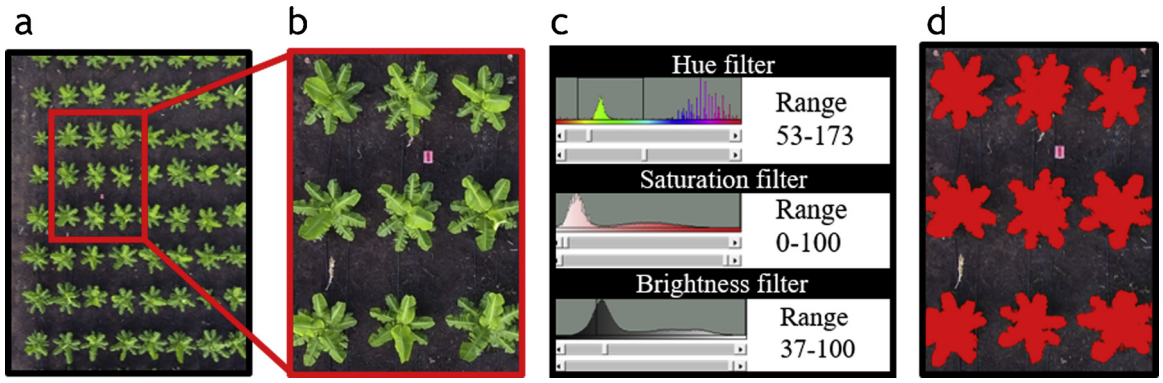

Fig. 1. Drone image analysis procedure. a) Original picture at 35 m above the ground, b) image cropped to retain nine central mats from a plot, c) HSB threshold selection for green pixels and d) filtered image with only green pixels selected shown in red. (For interpretation of the references to colour in this figure legend, the reader is referred to the web version of this article).

To compare CC values across measurement dates, the earliest CC pictures were used to exclude possible diurnal effects.

2.6.1.1. Canopy cover image analysis. ImageJ software (Abràmoff et al., 2004) was used to process images (Fig. 1). First, images of individual mats were cropped to a ground area of 6 m^2 to only retain the mat of interest, whilst plot images were cropped to retain the central nine mats of each plot (ground area of approx. 54 m^2). Each image was cropped four times. Second, CC was calculated based on colour segmentation according to HSB thresholding (Hue, Saturation, Brightness), where threshold ranges for H, S and B were determined for the green CC pixels. All pixels within these thresholds were set to 1 and the remaining pixels were set to 0. A noise reduction was applied so only pixel areas above a certain minimal pixel size were counted as green CC pixels. HSB threshold ranges and minimal pixel size were determined subjectively for each individual picture as lighting conditions in the field were not uniform and did not allow single HSB ranges to be applied to all pictures. The CC was then calculated as: $CC = 100 \times Green\ CC\ pixels/Total\ pixels$. To examine CC diurnal variation, a relative CC was calculated for each hour of image taking. The relative CC was calculated as $CC_{rel,i} = 100 \times CC_i/CC_{i=0}$; with $CC_{rel,i}$ being the relative CC (0–1) at time point i, CC_i being the absolute CC (%) at time point i and $CC_{i=0}$ being the absolute CC (%) of the first drone measurements of the day.

2.6.2. Leaf area index

The leaf area index was calculated from monthly collected growth parameters. The leaf area of individual leaves (LA_{leaf}) was calculated as follows:

$$LA_{leaf,i} = LL \times LW \times laf; \quad (3)$$

with *LL* and *LW* being the length and width of the leaf i, and *laf* being a leaf area factor (-). The *laf* was calculated following Nyombi et al. (2009), from leaves measured during destructive sampling (Fig. S3a). During development, leafs were numbered cumulatively and the LL and LW of each leaf was either measured during monthly growth measurement, at harvest or interpolated between LL and LW of measured leaves leading to a database with LL and LW for each developed leaf (figure S4.), showing the exponential nature of leaf area over time.

The total leaf area of a plant (LA_{plant}) was calculated by summing the area of all the present leaves as:

$$LA_{plant,\,calc} = \sum_{i=cumO}^{cumY} LA_{leaf,i} \quad (4)$$

with $LA_{leaf,i}$ is the leaf area of the i^{th} leaf as obtained from Eq. 3, *cumO* is the oldest cumulative leaf present and *cumY* is the youngest cumulative leaf present on a plant. Comparison of $LA_{plant,\,calc}$ with $LA_{plant,\,measured}$ for destructively sampled plants is shown in supplementary material (Fig. S3b). The total leaf area of an individual mat (LA_{mat}) was then calculated as the sum of the leaf area of C1 and its successor C2: $LA_{mat} = LA_{plant,C1} + LA_{plant,C2}$; whilst summing the leaf mat areas of all the nine plants within a plot led to the leaf area plot (LA_{plot}): $LA_{plot} = \sum_{i=1}^{n=9\ mats} LA_{mat}$. LAI_{plot} was then calculated by dividing LA_{plot} with its ground area (m^2).

2.6.3. Correction for plant death

In experiment 1, weak plants due to disease and other unknown factors, were replaced by sucker derived plants on 2017-09-21. The area of the diseased or replanted mats was excluded in further image analysis. The total area of the central plot was divided into nine squares corresponding to the ground area of the single mats. Empty and diseased mat positions were then blocked out, after which the CC was determined on the other plant positions (Fig. S2).

2.7. Statistical analysis

Field plots were the experimental units for the statistical analysis. As data were collected from the same plots over time, they constitute longitudinal repeated measures data. We used linear mixed models to analyze the effect of irrigation treatment on: soil moisture, CC growth, LAI evolution, and diurnal canopy cover variation. Differences in soil moisture, LAI and CC used WAP and treatment as fixed factors, and block and plot as random factors. Differences in diurnal CC variation between FI and RF plots used time (h) and treatment as fixed factors, whilst using block and plot as a random factors.

CC growth curves were obtained through nonlinear least squares (nls) regression on CC values obtained during the first drone flights of the day, to exclude a potential diurnal CC effect. Observations were average CC per plot level. Curve fitting through these points followed the standard logistic equation as follows:

$$CC_t = \frac{CC_{max}}{1 + \left(\frac{CC_{max} - CC_{ini}}{CC_{ini}}\right)e^{-rt}} \quad (5)$$

with CC_t being CC (%) at time t (WAP), CC_{max} being the max. CC (%), CC_{ini} being the initial CC at planting (%) and *r* being the CC growth rate (wk^{-1}). During regression, WAP was treated as a numeric variable. Residual plots and ANOVA comparison of fitted models were used to determine model selection.

To obtain CC-LAI curves for HG and GN, monthly LAI_{mat} values were compared with monthly CC estimates from the obtained logistic growth functions. A functional equation of the Lambert-Beer Law was fitted as:

$$CC = 100 \times [1 - exp^{(-b \times LAI_{mat})}] \quad (6)$$

with *b* being the extinction coefficient and LAI_{mat} being the leaf area

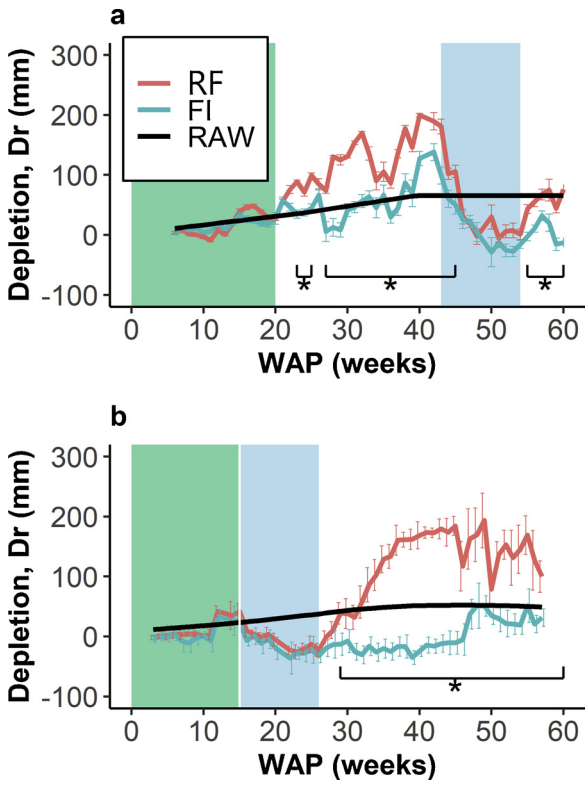

Fig. 2. Average soil moisture depletion (mm) versus time (WAP: weeks after planting) for two experiments. a) HG: Mchare - Huti Green. b) GN: Cavendish - Grande Naine. Under two irrigation regimes (FI: full irrigation and RF: rainfed). Green period: establishment period. Blue period: rainy season. Error bars denote mean ± standard deviation. '*' indicates a statistically significant ($p < 0.05$) difference between FI and RF. Black line indicates the Readily Available Water (RAW, 35 % of the Total Available Water). (For interpretation of the references to colour in this figure legend, the reader is referred to the web version of this article).

index (m^2 m^{-2}). To exclude a potential diurnal CC effect, CC values used were obtained during the first drone flights of the day. Observations were average CC per plot level.

Statistical analyses were performed in R version 3.4.3 (R Core Team., 2017). Linear mixed models were fitted using REML with the function lmer from the package nlme (Pinheiro et al., 2019). Plots were made using the package ggplot2 (Wickham, 2016). Nls regressions were performed using the package nls (R Core Team., 2017).

3. Results

3.1. Soil moisture depletion

During the establishment periods (0–20 WAP) soil moisture depletions did not differ significantly ($p > 0.05$) between FI and RF in both experiments except for GN at WAP 15 when FI plots were less depleted than RF plots (diff = 18.27 mm ± 8.69 mm, $p = 0.039$) (Fig. 2).

After the establishment period, differences in soil moisture closely followed the dry season.

In HG, soil moisture depletion in the RF plots first became significantly larger at 23 WAP (diff = 54.29 mm ± 19.25 mm, $p = 4.22e^{-3}$) until 45 WAP (diff = 67.62 mm ± 17.50 mm, $p = 8.81e^{-3}$). From 45 until 55 WAP soil moisture depletions were similar ($p > 0.05$). At 55 WAP, one week after the rainy season ended, RF plots became significantly more depleted than FI plots (diff = 45.80 mm ± 19.06 mm, $p = 0.015$) until the end of the growth trial (60 WAP [diff = 88.94 mm ± 19.06 mm, $p = 1.7e^{-4}$]). Soil moisture of the FI plots exceeded the RAW multiple times during the growing season, so moisture deficit could not fully be excluded in these plots.

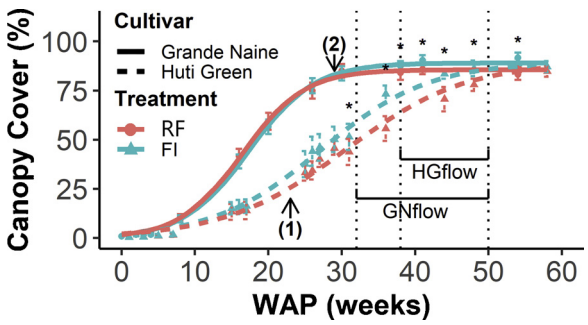

Fig. 3. Nonlinear least squares (nls) regression curves of canopy cover (CC: %) over time (WAP: weeks after planting) for two experiments (HG: Mchare - Huti Green, GN: Cavendish - Grande Naine) under two irrigation regimes (FI: full irrigation and RF: rainfed) Points denote actual average CC, error bars denote mean ± standard deviation as determined at plot level (n = 3 for HG and n = 4 for GN). HGflow indicates period of flowering of C1 in HG experiment. GNflow indicates period of flowering of cycle 1 (C1) in GN experiment; (1) denotes the onset of moisture divergence in HG experiment, whilst (2) indicates the onset of moisture divergence in GN experiment. '*' indicates a statistically significant ($p < 0.005$) difference between FI and RF. (For interpretation of the references to colour in this figure legend, the reader is referred to the web version of this article).

In GN, RF plots became significantly more depleted from 27 WAP (diff = 17.89 mm ± 8.69 mm, p = 0.04) until the end of the growth trial (57 WAP [diff = 100.07 mm ± 11.95 mm, $p < 2e^{-16}$]). In GN, soil moisture of the FI plots remained mostly below the RAW (except 12 WAP), so plants were considered non-stressed.

3.2. Canopy growth curves

Irrigation treatment had a significant effect on CC at plot level in both experiments ($p < 0.05$) (Fig. 3). For HG, CC was reduced significantly in the RF plots from 31 WAP (diff = 7.66 % ± 3.77 %, $p = 0.05$) (8 weeks after moisture divergence) to 48 WAP (diff = 8.50 % ± 3.77 %, $p = 0.04$). All nls parameters were significant ($p < 0.05$) in the regression analyses (Table 1). The growth rate (r) was reduced in the RF treatment (r = 0.12 ± 0.006, $p < 8.81e^{-9}$) whilst CC_{ini} and CC_{max} remained similar ($p = 0.2429$), leading to a significant CC divergence between 25 and 54 WAP corresponding to the dry season (Fig. 3 and Table 1). HG plots entered the dry season at 20 WAP (Fig. 2) when CC values were approx. 25 % and rapid canopy development was expected to start. CC divergence between treatments reached a maximum divergence at 36 WAP (diff = 17.59 % ± 3.77 %, $p = 2.89e^{-3}$), in the middle of the dry season. From 36 WAP, divergence between curves declined again and became negligible at 54 WAP ($p = 0.746$). For both RF and FI, CC growth continued significantly from 38 WAP to 50 WAP, the period of flowering of C1 plants.

For GN, CC was affected significantly from 38 WAP (diff = 3.54 % ± 1.14 %, $p = 0.008$) onwards (9 weeks after moisture divergence). The nls regression parameters r and CC_{max} were significantly affected by the RF treatment ($p < 6.8e^{-3}$). Differences in r were statistically significant, but lie very close to each other as shown by the overlapping 95 % confidence intervals (CI): 95 % CI [0.22; 0.25] for RF and 95 % CI [0.21; 0.24] for FI. CC_{max} differences were more pronounced: 95 % CI [83.99; 87.34] for RF and 95 % CI: [87.33; 90.91] for FI (Table 1). GN entered the dry season at 29 WAP, when CC values were approx. 85 % for both RF and FI, hence close to reaching the CC_{max} (Fig. 3). CC_{max}, or the stationary phase of the CC curve, was reached closely corresponding to flowering for C1 (32 WAP to 50 WAP).

3.3. Diurnal CC variation

Due to practical reasons (weather conditions, drone regulations and

Table 1
Canopy cover growth curves parameters for two experiments HG: Mchare Huti Green and GN: Cavendish Grande Naine under two irrigation regimes (FI: full irrigation and RF: rainfed). Growth curves follow the standard logistic regression and parameters were obtained through nonlinear least squares regression. Where parameters differed between RF and FI this is specified. Where no specification occurs, parameters were similar between drought and irrigated plots ($p < 0.05$).). r-RF and r-FI denote the significantly different CC growth rates in RF and FI plots, whilst CC_{max}-RF and CC_{max}-FI denote the significantly different CC_{max} values in RF and FI plots ($p < 0.005$). CC_{ini} is similar in both treatments..

Huti Green regression parameters

Parameter	Abbrev.	Unit	Value	SE	95 % CI	t-value	p-value	significance
Initial canopy cover	CC_{ini}	%	2.13	0.346	[1.55; 2.83]	6.15	1.84E-08	***
Growth rate†	r							
Growth rate drought	*r-RF*	–	0.12	0.006	[0.11; 0.14]	19.57	< 2e-16	***
Growth rate irrigated	*r-FI*	–	0.14	0.007	[0.13; 0.15]	20.03	< 2e-16	***
Maximum canopy cover	CC_{max}	%	89.59	1.526	[86.68; 92.77]	58.71	< 2e-16	***

Grande Naine regression parameters

Parameter	Abbrev.	Unit	Value	SE	95 % CI	t value	p value	significance
Initial canopy cover	CC_{ini}	%	1.71	0.205	[1.34; 2.13]	8.35	1.85E-12	***
Growth rate‡	r							
Growth rate RF	*r-RF*	–	0.24	0.008	[0.22; 0.25]	31.04	< 2e-16	***
Growth rate FI	*r-FI*	–	0.23	0.007	[0.21; 0.24]	31.00	< 2e-16	***
Maximum canopy Cover§	CC_{max}	%						
Maximum Canopy cover RF	*CC_{max}-RF*		85.65	0.840	[83.98; 87.34]	101.94	< 2e-16	***
Maximum Canopy Cover FI	*CC_{max}-FI*		89.10	0.893	[87.33; 90.91]	99.80	< 2e-16	***

† Significant different growth rates between RF and FI plots for Huti Green ($p < 0.05$).
‡ Significant different growth rates between RF and FI plots for Grande Naine ($p < 0.05$).
§ Significant different maximum canopy cover between RF and FI plots for Grande Naine ($p < 0.05$).

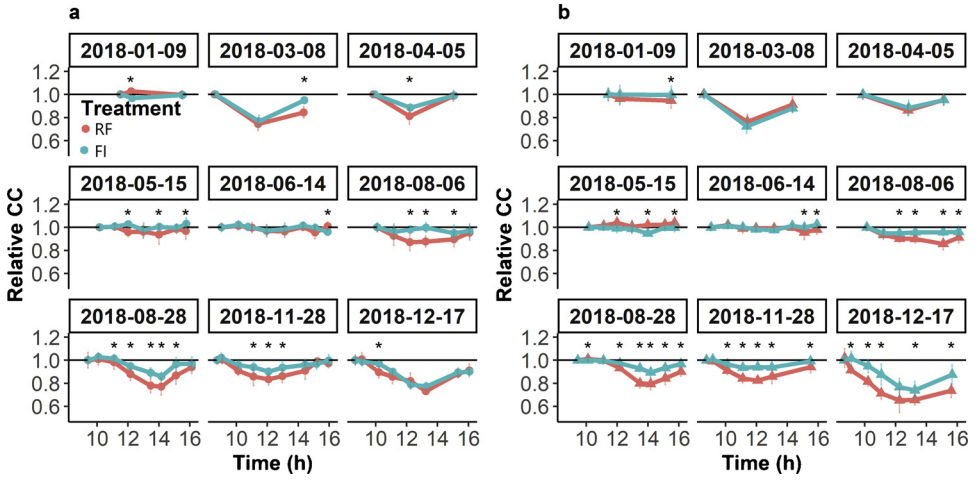

Fig. 4. Relative canopy cover (CC_{rel}) evolution during the day for different dates of drone flights. a) Experiment 1, HG: Mchare - Huti Green and b) Experiment 2, GN: Cavendish - Grande Naine, under two irrigation regimes (FI: full irrigation and RF: rainfed). Points denote average CC_{rel}, error bars denote ± standard deviation as determined on plot level (n = 3 for HG and n = 4 for GN). "*" notes when CC_{rel} of RF is significantly lower than CC_{rel} of FI ($p < 0.05$ and 95 % CI do not overlap). (For interpretation of the references to colour in this figure legend, the reader is referred to the web version of this article).

flight scheduling) pictures of CC could not always be taken at a hourly interval at each day, yet CC was always determined at minimally three time points (Fig. 4).

Hour of measurement influenced relative CC (CC_{rel}) values significantly at all measurement dates in both cultivars (all $p < 0.05$), but the effect of time on CC_{rel} varied by date. Although significant, time point had a weak effect on CC_{rel} in January, May and June for both HG and GN as CC_{rel} during the day remained close to 1 (Fig. 4). Time effects were more pronounced in March, April, August, November and December 2018 as curves show a more pronounced deviation from the 1 line.

CC_{rel} was compared against weather parameters, as similar patterns emerged at the same date in both HG and GN experiments. Daily ET_0 was highly correlated ($R^2 > 0.86$) with solar radiation, relative humidity and vapor pressure deficits (other indicators of evaporative demand). Dates with more pronounced CC_{rel} reduction (in both RF and FI) (Fig. 4) were characterized by a higher ET_0 (Fig. 5a). Overall a clear pattern emerges. Under high ET_0 (> 3 mm day^{-1}), CC reduces from morning values and reaches minimal values around noon, after which it increases again in the afternoon (Fig. 4).

Soil moisture deficits had an additional effect on CC_{rel} patterns, depending on the prevailing ET_0 (Fig. 5b). When ET_0 is low (< 3 mm day^{-1}), there is no additional folding with increasing depletion (p = 0.7938). Only when ET_0 increases (> 3 mm day^{-1}), do increasing depletion values exacerbate the folding ($p = 8.72e^{-3}$). At low ET_0 (< 3 mm day^{-1}), the CC_{rel} is therefore similar in RF and FI, whilst under high ET_0 (> 3 mm day^{-1}), increasing depletion leads to a lower CC_{rel}.

3.4. CC-LAI curve determination

3.4.1. Leaf area factor

Destructively sampling plants allowed to establish a laf of 0.66 ($\pm$ 0.018, $p < 2e^{-16}$) for HG, while laf of GN was determined to be 0.75 ($\pm$ 0.012, $p < 2e^{-16}$). Single laf values were used for calculating LA_{leaf} values, as no pattern emerged with increasing leaf size (Fig. S3a).

3.4.2. LAI evolution

Irrigation treatment had a significant effect on LAI_{plant} and LAI_{mat} in

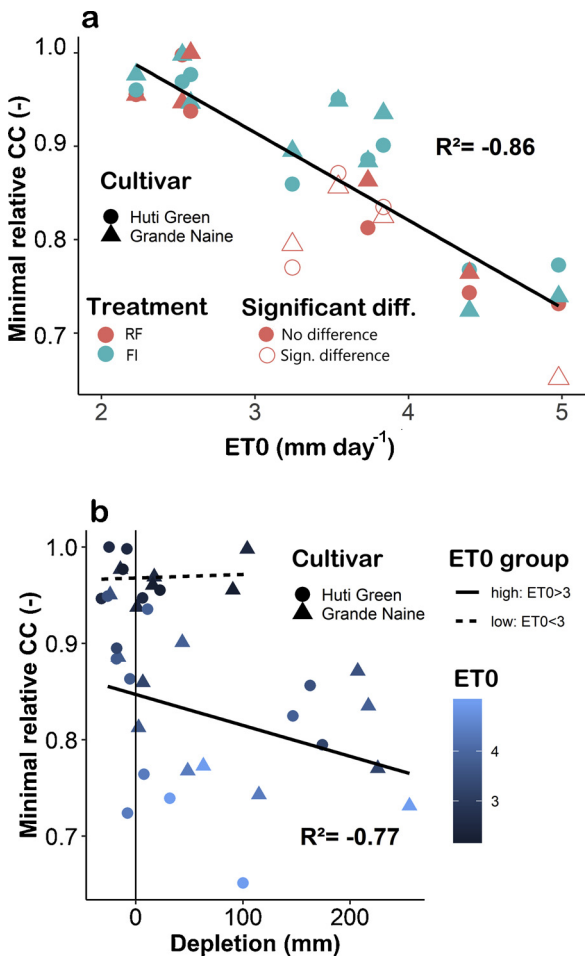

Fig. 5. Minimal daily relative canopy cover (CC_{rel}) for different drone flying dates compared against a) daily reference evapotranspiration: ET_0 (mm day^{-1}) and b) soil moisture depletion on plot level (mm) for two experiments (HG: Mchare - Huti Green, GN: Cavendish - Grande Naine) under two irrigation regimes (FI: full irrigation and RF: rainfed). (For interpretation of the references to colour in this figure legend, the reader is referred to the web version of this article).

both experiments (Fig. 6). In HG, LAI_{plant} and LAI_{mat} were significantly reduced by drought from 31 WAP onwards ($p < 0.05$). Fungus pruning started at 55 WAP, after which LAI could no longer be calculated due to the big size of the plants.

In GN, LAI_{plant} of C1 increased steadily until the first onset of flowering (32 WAP), after which there was a big drop in LAI_{plant} of C1 due to leaf pruning at 37 WAP (P3), whereby the lowest six leaves were cut from all plants in both FI and RF (Fig. 6). LAI_{plant} of C1 was significantly reduced in the RF plots from 42 WAP onwards ($p = 0.009$), whilst LAI_{plant} of C2 was affected from 46 WAP ($p = 1.65e^{-5}$). LAI_{mat} behaved similarly and started diverging from 42 WAP onwards ($p = 5e^{-4}$).

As such, LAI in both experiments reacted to moisture deficit at about 8–9 weeks after soil moisture divergence, similarly as CC values.

3.5. CC-LAI curves

LAI_{mat} values were used to create CC-LAI curves for both cultivars, which follow an exponential function (Fig. 7).

CC and LAI were accurately fitted by the Lambert-Beer equation for both cultivars. HG had significantly lower extinction coefficient ($b = 0.51 \pm 0.0038$, $p < 2e^{-16}$) than GN ($b = 0.67 \pm 0.0046$, $p < 2e^{-16}$) showing that at a similar LAI, a lower CC is reached in HG.

4. Discussion

4.1. Canopy cover growth over time

Total precipitation received during the C1 growth cycle (lasting over 60 WAP) was about 1403 mm for HG, and 1607 mm for GN. Total amounts might be sufficient for optimal banana production (1100–2650 mm yr^{-1}) but not evenly spread, as there were two distinct rainy seasons interrupted by dry spells of more than two months implying the need for irrigation (Robinson and Alberts, 1986; Van Asten et al., 2011; Varma and Bebber, 2019). FI plots received 3416 mm (HG) and 4400 mm (GN) over the entire growing season, compared to RF plots which received 1770 mm (HG) and 1340 mm (GN) during the first 4 MAP to establish the fields. As growth was significantly reduced in RF plots, irrigation proved necessary in Arusha for both experiments.

CC in both experiments was significantly affected by soil moisture deficit (Fig. 3), but timing and severity occurred at different developmental stages in the experiments (Fig. 2). Divergence of soil moisture in HG started at the start of the exponential growth phase (23 WAP) when CC values were approx. 25 %. As drought coincided with the beginning of the exponential growth phase absolute CC differences were more pronounced, and became first significant (diff = 7.66 % ± 3.77, $p = 0.05$) at around 8 weeks after the onset of soil moisture differences (31 WAP). At 36 WAP, in the middle of the dry season, CC in FI plots was 17 % (± 3.77) larger than the RF plots ($p = 1.65e^{-4}$).

For GN, the absolute effect of drought on CC was less, as CC reached about 85 % at moisture divergence (29 WAP onwards), and most of the leaves of C1 had already formed so close to flowering. CC differences between RF and FI plots became significantly different from 38 WAP onwards (diff = 3.54 % ± 1.15), about 9 weeks after soil moisture values started diverging indicating moisture deficit to have an effect on the CC even close to flowering.

CC as such reacted quickly to moisture deficit in both experiments. Drought induces stomatal closure, reducing transpiration, photosynthesis, thereby reducing leaf area and leaf emission rate (Kallarackal et al., 1990; Thomas and Turner, 1998; Taiz and Zeiger, 2002; Carr, 2009) both playing a role in CC formation. As new leaves emerge at the top of the pseudostem, and newly formed leaves cover older ones, a reduction in leaf appearance rate and a corresponding decrease in leaf area of new leaves due to moisture deficit, will have a significant effect on the CC, depending on the severity and timing of drought. Indeed, CC and LAI (Figs. 3 and 6) were both significantly reduced by moisture deficits in both experiments.

Logistic growth curves accurately captured CC growth for both HG and GN although CC values were slightly overestimated (1–2 %) at the beginning of the growing season for both experiments (Fig. 3). Over the full growing season, this initial overestimation is negligible.

For HG, CC growth curves for RF and FI deviated more and hence a CC divergence from optimal values during the vegetative stage can therefore be a good indicator of moisture deficit. Similar CC_{max} values were reached due to the occurrence of the rainy season between 43 and 54 WAP, allowing mats in RF plots to reach LAI_{mat} values leading to near maximum CC (Fig. 7). So even though LAI_{mat} differed significantly (Fig. 6), CC did not differ significantly (Fig. 3 and Fig. 7).

For GN, the growth rate r was slightly increased under moisture deficit, but this statistically significant difference leads to very small CC growth curve differences. CC_{max} differed significantly which is due to differential leaf formation in C1 and C2 after soil moisture divergence (Fig. 6). Even the last developed leaves before flowering of C1, and leaves of C2 therefore have an effect on overall CC, albeit a smal absolute effect given the exponential nature of the CC-LAI curve (Fig. 7).

Similar CC_{max} values of approx. 90 % were reached in both experiments under FI, being close to values in other crops under optimal spacing: peach 93 % (McClymont et al., 2005), apple 93 % (McClymont et al., 2005), Amaranthus 95 % (Bello and Walker, 2017), cabbage 95 % (Wellens et al., 2013), vining pea 95 % (Paredes and Torres, 2016),

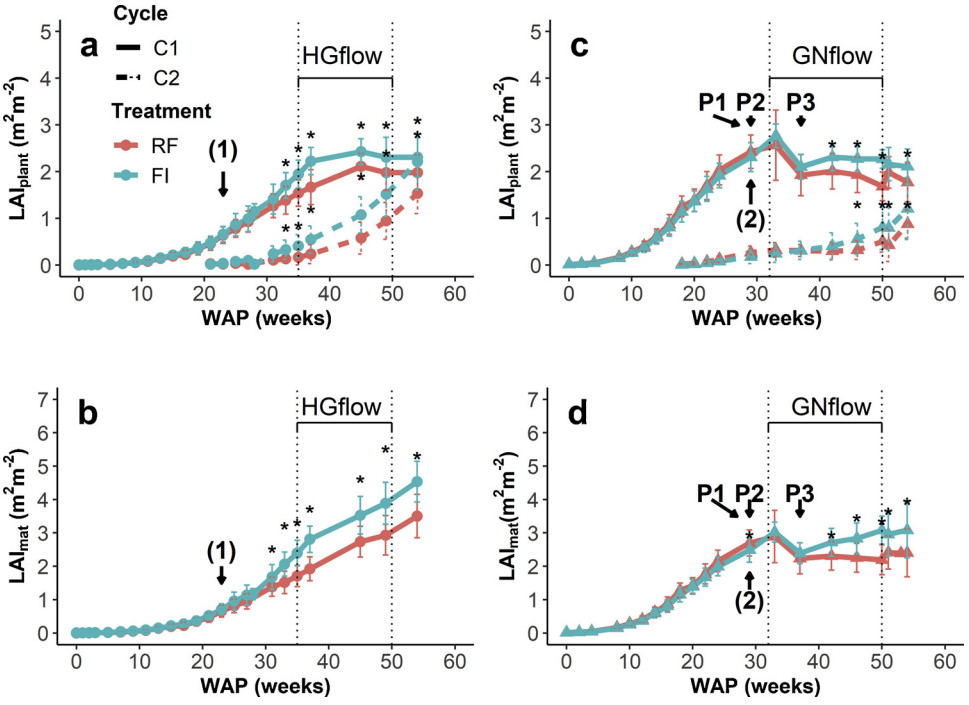

Fig. 6. LAI evolution for two experiments (HG: Mchare - Huti Green, GN: Cavendish - Grande Naine) under two irrigation regimes (FI: full irrigation and RF: rainfed). **a)** LAI_{plant} values for HG cycle 1 (C1) and cycle 2 (C2), **b)** LAI_{mat} values for HG, composed of both cycles, **c)** LAI_{plant} values for GN cycle 1 (C1), **d)** LAI_{mat} values for GN, composed of both cycles. Points denote average LAI, error bars denote ± standard deviation as determined on plot level (n = 3 for HG and n = 4 for GN). P1, P2 and P3 indicate the different leaf pruning events. GNflow indicates the period of flowering of C1 in GN; HGflow indicates the period of flowering of C1 in HG. (1) indicates the onset of moisture divergence in experiment 1, whilst (2) indicates the onset of moisture divergence in experiment 2. '*' indicates a statistically significant ($p < 0.05$) difference between LAI in FI and RF plots. (For interpretation of the references to colour in this figure legend, the reader is referred to the web version of this article).

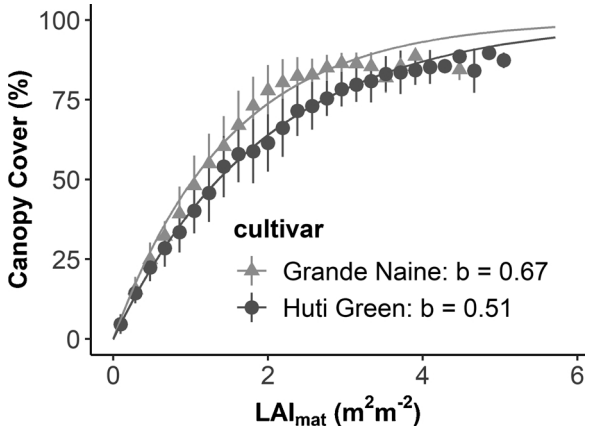

Fig. 7. Relationship between leaf area index (LAI_{mat}) and canopy cover (CC) for two banana cultivars (HG: Huti Green, GN: Grande Naine). Fitted lines are regressed on plot data (points) until flowering of Cycle 1 in HG (n = 3) and GN (n = 4). Extinction coefficients are significantly different ($p < 0.05$). (For interpretation of the references to colour in this figure legend, the reader is referred to the web version of this article).

cotton 90 % (Farahani et al., 2009), maize 90–95 % (Hsiao et al., 2009). CC_{max} values of 100 %, while theoretically possible, are rarely reached even with dense planting.

Commonly used densities of HG is 2 × 2 m (2500 plants ha^{-1}) and of GN is 3 × 2.5 m (1333 plants ha^{-1}) respectively, and differed from the used planting density (1667 plants ha^{-1}). Different CC curves would be obtained with these spacings, where CC curves (Fig. 3) would shift upward for HG (faster CC growth), and downward for GN (slower CC growth). Then, differences between cultivar CC curves might not be as pronounced as now. Additional research should look at the CC evolution in plantations under different densities planted at the same time to see the density effect on CC growth curves.

4.2. Diurnal CC pattern

CC showed a significant diurnal pattern on days characterized by high evaporative demands ($ET_0 > 3$ mm day^{-1}) in both experiments (Figs. 4 and 5). Overall a clear pattern emerged. Under high ET_0 (> 3 mm day^{-1}), CC reduces from morning values and reaches minimal values around noon, after which it increases again in the afternoon (Fig. 4). The larger the daily ET_0, the larger this CC reduction at noon (Fig. 5a). On days of high ET_0, soil moisture depletion in RF plots significantly increased the CC reduction at midday ($p < 0.05$) compared to FI plots (Fig. 5b). Hence, both environmental stimuli and the soil moisture deficit status play a role in diurnal CC patterns. We hypothesize this CC pattern to occur due to leaf folding of banana plants.

Leaf folding occurs in well-watered, non-stressed banana plants and typically follows a diurnal rhythm with leaf halves bounding a single plane aligning the midrib during the night and early morning, becoming more vertical (fold downward) during periods of high evaporative demand and returning to their original position (fold upward) in the late afternoon (Milburn et al., 1990; Thomas and Turner, 1998; Turner and Thomas, 1998; Turner et al., 2007; Carr, 2009).

Leaf folding in response to drought is still debated, but some research suggests diurnal leaf folding to be more pronounced under drought (Milburn et al., 1990; Thomas and Turner, 1998; Turner and Thomas, 1998), whilst others refute this claim (Lu et al., 2002). Our results indicate leaf folding indeed is increased under drought, given ET_0 is high enough.

Other plants also exhibit leaf folding at field scale under drought. Maize, rice, wheat, and sorghum (amongst other grasses) roll their lamina upward transversally to the mid rib under stress conditions due to a drop in water potential (turgor) in the leaf. Leaf "rolling" results from varying degrees of dehydration in different cross sections of the rolled leaf (Kadioglu et al., 2012). Rolling in maize leaves follows a diurnal pattern whereby maximum closure is reached at solar noon during days of high evaporative demand, but not present in well-watered plants. Leaf rolling in grasses is therefore a visible indication of moisture deficit and also present at the canopy level (Baret et al., 2018).

In banana, leaf folding results from differential turgor of cells in the leaf pulvinar bands, following a similar process as changes in stomatal aperture which are being controlled by the turgor of the guard cells (Satter and Galston, 1981; Turner et al., 2007). Diurnal leaf folding in banana may therefore be due to changes in leaf turgor pressure on a diurnal scale. Zimmermann et al. (2010), studied the effects of

environment and irrigation on leaf turgor pressure using a leaf patch clamp pressure probe on diurnal timescales. They showed leaf turgor varied diurnally in both irrigated and non-irrigated plants plants. Generally, leaf turgor pressure declined from morning values, reached a minimal value around noon after which turgor increased again in the late afternoon and during the night. On days with high evaporative demands, turgor pressure drops were more pronounced, indicating leaf turgor pressure reacted directly to the environment. Under optimal irrigation, turgor pressure dropped less and recovered during the night, whilst under sub-optimal irrigation turgor pressure drops were more pronounced and did not recover. They concluded turgor pressure amplitudes and stabilization time might therefore be indicators of moisture deficit on a diurnal scale (Zimmermann et al., 2010).

Given our findings and the fact leaf turgor plays a role in leaf folding, we hypothesize the diurnal CC pattern to reflect these diurnal turgor pressure pattern in a leaf. At high evaporative demands (possibly exacerbated by soil drought), leaf turgor drops, resulting in folding of the leaves and closing of the stomata. We hypothesize the bigger the evaporative demand, and the more soils are moisture depleted, the more leaf turgor is affected leading to a more pronounced leaf folding and a more pronounced diurnal CC pattern. Further research is needed to prove this hypothesis.

CC diurnal patterns by themselves are not good indicators of moisture deficit, as they do not occur when ET_0 is low and occur even in well irrigated plots when ET_0 is high. However, comparison of irrigated with non-irrigated plots on days of high ET_0 could indicate moisture deficit due to an increased and prolonged CC drop at midday.

This diurnal CC pattern needs to be taken into account when creating CC curves for crop growth modelling. CC pictures need to be taken early in the morning (< 8 h) or in the evening (> 18 h) to reduce the CC variation and make use of optimal light conditions.

4.3. CC-LAI relationship

As banana cultivars are phenologically diverse, it is necessary to determine a laf to correctly determine the LA_{leaf} for each cultivar. Laf was 0.66 ($\pm$ 0.004, $p < 2.2e^{-16}$) for HG, and 0.75 ($\pm$ 0.004, $p < 2.2e^{-16}$) for GN. These values are in the range of published laf values (Obiefuna and Ndubizu, 1979; Blomme and Tenkouano, 1998; Nyombi et al., 2009). Using the laf for HG and GN, LAI_{mat} values for HG and GN ranged between 0 m^2m^{-2} and 5 m^2m^{-2} (Fig. 6 and Fig. 7) corresponding with the LAI range noted in commercial plantations (Turner, 1972, 1998; Turner et al., 2007).

CC-LAI relationships were obtained for both cultivars with LAI_{mat} being composed of both C1 and C2 (Fig. 7). The CC-LAI relationship was exponential as in wheat, Triticale and maize (Hsiao et al., 2009; Nielsen et al., 2012). At a similar spacing, CC-LAI curves differed significantly ($p = 4.731e^{-10}$) between the two cultivars. HG had a significantly lower extinction coefficient ($b = 0.52 \pm 0.006$) than GN ($b = 0.67 \pm 0.004$), indicating that at similar LAI values a lower CC will be obtained for HG. This can be due to the ploidy of the cultivars as diploids (HG) exhibit more erect leaves than triploids (GN). At similar LAI values, erect leaves cover less ground than more horizontal leaves. This remains speculation, as to test whether it is a ploidy effect, rather than a cultivar effect, more cultivars need to be tested.

Overall, CC, LAI and corresponding CC-LAI curves are influenced by cultivar, plant spacing, mother-daughter relationships and management and environments (Turner, 1998; Turner et al., 2007; Wellens et al., 2013). Hence a single CC-LAI curve cannot be proposed for banana (*Musa* spp.). Changing plant density to optimal densities for HG (2 m × 2 m) and GN (2.5 m × 3 m) would shift the CC-LAI curve upward for HG, and downward for GN, bringing them closer together.

5. Conclusion

CC growth, and growth curves where significantly affected by moisture deficit, indicating CC growth over time can be used as an indicator of moisture deficit in plantations. Over a growing season, both CC and LAI were significantly reduced 8–9 weeks after moisture divergence between the RF and FI plots in both experiments. Solely using CC as an indicator of growth, however does not allow to separate the effect of drought between the different cycles, and therefore CC curves over time can only be used as indicators of the total plantation reaction to drought. When separating growth of the different cycles, LAI is of better use as this can more easily be separated between mother and daughter plants.

On a daily timescale LAI remains stable, whereas CC varies according to evaporative demands and moisture depletion. At low evaporative demands, CC did not vary significantly. At high evaporative demands CC was reduced at midday, with reductions being increased by increasing soil moisture depletion. In view of this diurnal CC pattern, we hypothesize CC drops to reflect the leaf turgor pressure, which has proven to vary similarly on a diurnal timescale and plays a role in leaf folding. More research is however needed to prove this hypothesis. Daily monitoring of CC at morning compared to midday might be an indicator of soil moisture deficit if a reference plot that is fully irrigated is present.

CC-LAI curves for both cultivars followed the Lambert-Beer law, with both cultivars having significant different extinction coefficients. CC-LAI curves are expected to depend on the plant spacing and used cultivar, as the difference in extinction coefficient might be due to the different leaf physiology of the used cultivars.

In summary, CC as an indicator of growth offers potential in monitoring soil moisture deficit in banana plantations.

CRediT authorship contribution statement

Bert Stevens: Conceptualization, Data curation, Formal analysis, Funding acquisition, Investigation, Methodology, Resources, Software, Visualization, Writing - original draft, Writing - review & editing. **Jan Diels:** Conceptualization, Formal analysis, Funding acquisition, Investigation, Methodology, Project administration, Resources, Supervision, Writing - original draft, Writing - review & editing. **Eline Vanuytrecht:** Conceptualization, Supervision. **Allan Brown:** Conceptualization, Funding acquisition, Project administration, Resources, Supervision, Writing - original draft. **Stanley Bayo:** Investigation. **Alvin Rujweka:** Resources. **Emmanuel Richard:** Investigation. **Patrick Alois Ndakidemi:** Conceptualization, Methodology, Project administration, Resources, Supervision, Visualization, Writing - original draft. **Rony Swennen:** Conceptualization, Formal analysis, Funding acquisition, Methodology, Project administration, Resources, Supervision, Writing - original draft, Writing - review & editing.

Declaration of Competing Interest

The authors declare that they have no known competing financial interests or personal relationships that could have appeared to influence the work reported in this paper.

Acknowledgement

This study was conducted at the joint research farm of the Nelson Mandela African Institute of Science and Technology (NM-AIST) and the International Institute of Tropical Agriculture (IITA), and was supported by the Belgian VLIR-UOS, through a VLADOC scholarship. The authors are also grateful to all donors who supported this work through their contributions to the CGIAR Fund (https://www.cgiar.org/funders/) and in particular to the CGIAR Research Program for Roots, Tubers and Bananas (CRP-RTB). E. Vanuytrecht received post-doc funding from the Flemish Research Foundation (FWO). We thank

the many people involved in fieldwork and technical assistance: Stanley John Bayo, Emmanuel Richard Nasolwa, Erick Wangaely, Salim Ramadhani and Joshua Jackson for the maintenance of the field; Hassan Mduma and Veronica Massawe for their practical guidance and Scola Ponera for administrative support.

Appendix A. Supplementary data

Supplementary material related to this article can be found, in the online version, at doi:https://doi.org/10.1016/j.scienta.2020.109328.

References

Abele, S., Twine, E.E., Legg, C., 2007. Food Security in Eastern Africa and the Great Lakes Technical Report.

Abràmoff, M.D., Magalhães, P.J., Ram, S.J., 2004. Image processing with imageJ. Biophotonics Int.

Adhikari, U., Nejadhashemi, A.P., Woznicki, S.A., 2015. Climate change and eastern Africa: a review of impact on major crops. Food Energy Secur. 4 (2), 110–132. https://doi.org/10.1002/fes3.61.

Allen, R.G., Pereira, L.S., Raes, D., Smith, M., 1998. FAO 56: crop Evapotranspiration (guidelines for computing crop water requirements). FAO Irrig. Drain. Pap. 300 (56), 300. https://doi.org/10.1016/j.eja.2010.12.001.

Baret, F., Madec, S., Irfan, K., Lopez, J., Comar, A., et al., 2018. Leaf-rolling in maize crops : from leaf scoring to canopy-level measurements for phenotyping. J. Exp. Bot. 69 (10), 2705–2716. https://doi.org/10.1093/jxb/ery071.

Bello, Z.A., Walker, S., 2017. Evaluating AquaCrop model for simulating production of amaranthus (Amaranthus cruentus) a leafy vegetable, under irrigation and rainfed conditions. Agric. For. Meteorol 247 (February), 300–310. https://doi.org/10.1016/j.agrformet.2017.08.003.

Blomme, G., Tenkouano, A., 1998. Effect of plant age and ploidy on estimated and actual leaf area of banana plants. Infomusa 7 (2), 6–7.

Boesveld, H., Zisengwe, L.S., Yakami, S., 2011. Drip Planner Chart: a simple irrigation scheduling tool for smallholder drip farmers. Irrig. Drain. Syst. Eng. 25 (4), 323–333. https://doi.org/10.1007/s10795-012-9127-4.

Carr, M.K.V., 2009. The water relations and irrigation requirements of Banana (Musa spp.). Exp. Agric. 45 (1), 333–371. https://doi.org/10.1017/S0014479713000288.

FAO, 2012. GAEZ: global agro-ecological zones. Food Agric. Organ.

FAO, 2018. The Future of Food and Agriculture – Alternative Pathways to 2050. Rome.

FAOSTAT, 2019. Banana and Plantain Production Data. http://www.fao.org/faostat/en/#data/.

Farahani, H.J., Izzi, G., Oweis, T.Y., 2009. Parameterization and evaluation of the aquacrop model for full and deficit irrigated cotton. Agron. J. 101 (3), 469–476. https://doi.org/10.2134/agronj2008.0182s.

Fortescue, J.A., Turner, D.W., Romero, R., 2011. Evidence that banana (Musa spp.), a tropical monocotyledon, has a facultative long-day response to photoperiod. Funct. Plant Biol. 38 (11), 867–878. https://doi.org/10.1071/FP11128.

Grieser, J., Gommes, R., Bernardi, M., 2006. New LocClim - the Local Climate Estimator of FAO. Geophys. Res. Abstr.

Hsiao, T.C., Heng, L., Steduto, P., Rojas-Lara, B., Raes, D., et al., 2009. Aquacrop-The FAO crop model to simulate yield response to water: III. Parameterization and testing for maize. Agron. J. 101 (3), 448–459. https://doi.org/10.2134/agronj2008.0218s.

Hunter, M.C., Smith, R.G., Schipanski, M.E., Atwood, L.W., Mortensen, D.A., 2017. Agriculture in 2050: recalibrating targets for sustainable intensification. Bioscience 67 (4), 386–391. https://doi.org/10.1093/biosci/bix010.

IUSS Working Group WRB, 2014. World reference base for soil resources 2014. International Soil Classification System for Naming Soils and Creating Legends for Soil Maps.

Jennings, S.B., Brown, N.D., Sheil, D., 1999. Assessing forest canopies and understorey illumination: canopy closure, canopy cover and other measures. Forestry 72 (1), 59–73. https://doi.org/10.1093/forestry/72.1.59.

Kadioglu, A., Terzi, R., Saruhan, N., Saglam, A., 2012. Current advances in the investigation of leaf rolling caused by biotic and abiotic stress factors. Plant Sci. 182, 42–48. https://doi.org/10.1016/j.plantsci.2011.01.013.

Kallarackal, J., Milburn, J., Baker, D., 1990. Water relations of the banana. III. Effects of controlled water stress on water potential, transpiration, photosynthesis and leaf growth. Aust. J. Plant Physiol. 17 (1), 79. https://doi.org/10.1071/PP9900079.

Lu, P., Woo, K.-C., Liu, Z.-T., 2002. Estimation of whole-plant transpiration of bananas using sap flow measurements. J. Exp. Bot. 53 (375), 1771–1779. https://doi.org/10.1093/jxb/erf019.

McClymont, L., Goodwin, I., O'Connell, M.G., Whitfield, D.M., 2011. Variation in within-block orchard canopy cover - Implications for crop water requirement and irrigation management. Acta Hortic. 889 (2005), 233–240.

Milburn, J.A., Kallarackal, J., Baker, D.A., 1990. Water relations of the banana. I. Predicting the water relations of the field-grown banana using the exuding latex. Aust. J. Plant Physiol. 17 (1), 57–68. https://doi.org/10.1071/PP9900057.

Nielsen, D.C., Miceli-Garcia, J.J., Lyon, D.J., 2012. Canopy cover and leaf area index relationships for wheat, triticale, and corn. Agron. J. 104 (6), 1569–1573. https://doi.org/10.2134/agronj2012.0107n.

Nyombi, K., Van Asten, P.J.A., Leffelaar, P.A., Corbeels, M., Kaizzi, C.K., et al., 2009. Allometric growth relationships of East Africa highland bananas (Musa AAA-EAHB) cv. Kisansa and Mbwazirume. Ann. Appl. Biol. 155 (3), 403–418. https://doi.org/10.1111/j.1744-7348.2009.00353.x.

Obiefuna, J.C., Ndubizu, T.O., 1979. Estimating leaf area of plantain. Sci. Hortic. (Amsterdam) 11 (June), 31–36.

Paredes, P., Torres, M.O., 2016. Parameterization of AquaCrop model for vining pea biomass and yield predictions and assessing impacts of irrigation strategies considering various sowing dates. Irrig. Sci. 1, 1–14. https://doi.org/10.1007/s00271-016-0520-x.

Perrier, X., Jenny, C., Bakry, F., Karamura, D., Kitavi, M., et al., 2018. East African diploid and triploid bananas: a genetic complex transported from South-East Asia. Ann. Bot. 123 (1), 1–18. https://doi.org/10.1093/aob/mcy156.

Pinheiro, J., Bates, D., DebRoy, S., Sarkar, D., Team, R.C., 2019. nlme: Linear and Nonlinear Mixed Effects Models. https://cran.r-project.org/package=nlme.

R Core Team, 2017. R: a Language and Environment for Statistical Computing.

Robinson, J.C., Alberts, A.J., 1986. Growth and yield Responses of Banana (Cultivar' Williams') to drip irrigation under Drought and Normal Rainfall Conditions in the Subtropics. Sci. Hortic. (Amsterdam). 30, 187–202. https://doi.org/10.1016/0304-4238(86)90097-X.

Robinson, J.C., Galán Saúco, V., 2010. Bananas and Plantains, second edition. .

Satter, R.L., Galston, A.W., 1981. Mechanism Of Control Of Leaf Movements. Annu. Rev. Plant Physiol. Plant Mol. Biol. 32, 83–110.

Taiz, L., Zeiger, E., 2002. Plant Physiology.

Thomas, D.S., Turner, D.W., 1998. Leaf gas exchange of droughted and irrigated banana cv. Williams (Musa spp.) growing in hot, arid conditions. J. Hortic. Sci. Biotechnol. 73 (3), 419–429. https://doi.org/10.1080/14620316.1998.11510994.

Turner, D.W., 1972. Dry matter production, leaf area and growth analvsis. Aust. J. Exp. Agric. Anim. Husb. 12, 216–224.

Turner, D.W., 1998. Ecophysiology of bananas: the generation and functioning of the leaf canopy. Acta Hortic. 490, 211–221.

Turner, D.W., Thomas, D.S., 1998. Measurements of plant and soil water status and their association with leaf gas exchange in banana (Musa spp.): A laticiferous plant. Sci. Hortic. (Amsterdam) 77 (3–4), 177–193. https://doi.org/10.1016/S0304-4238(98)00168-X.

Turner, D.W., Fortescue, J.A., Thomas, D.S., 2007. Environmental physiology of the bananas (Musa spp.). Brazilian J. Plant Physiol. 19 (4), 463–484. https://doi.org/10.1590/S1677-04202007000400013.

United Nations, 2019. World Population Prospects 2019.

USDA, 1999. Soil Taxonomy: A Basic System of Soil Classification for Making and Interpreting Soil Surveys, 2nd editio. .

Van Asten, P.J.A., Fermont, A.M., Taulya, G., 2011. Drought is a major yield loss factor for rainfed East African highland banana. Agric. Water Manag. 98 (1), 541–552. https://doi.org/10.1016/j.agwat.2010.10.005.

Varma, V., Bebber, D.P., 2019. Climate change impacts on banana yields around the world. Nat. Clim. Chang. 1–9. https://doi.org/10.1038/s41558-019-0559-9.

Wairegi, L.W.I., Van Asten, P.J.A., Tenywa, M.M., Bekunda, M.A., 2010. Abiotic constraints overide biotic constraints in East African highland banana systems. F. Crop. Res. 117 (1), 146–153. https://doi.org/10.1016/j.fcr.2010.02.010.

Weiss, M., Baret, F., Smith, G.J., Jonckheere, I., Coppin, P., 2004. Review of methods for in situ leaf area index (LAI) determination Part II. Estimation of LAI, errors and sampling. Agric. For. Meteorol. 121 (1–2), 37–53. https://doi.org/10.1016/j.agrformet.2003.08.001.

Wellens, J., Raes, D., Traore, F., Denis, A., Djaby, B., et al., 2013. Performance assessment of the FAO AquaCrop model for irrigated cabbage on farmer plots in a semi-arid environment. Agric. Water Manag. 127, 40–47. https://doi.org/10.1016/j.agwat.2013.05.012.

Wickham, H., 2016. ggplot2: Elegant Graphics for Data Analysis. https://ggplot2.tidyverse.org.

Zimmermann, U., Rüger, S., Shapira, O., Westhoff, M., Wegner, L.H., et al., 2010. Effects of environmental parameters and irrigation on the turgor pressure of banana plants measured using the non-invasive, online monitoring leaf patch clamp pressure probe. Plant Biol. 12 (3), 424–436. https://doi.org/10.1111/j.1438-8677.2009.00235.x.